2022 European Control Conference (ECC)
July 12-15, 2022. London, United Kingdom

Event-Triggered Eco-Driving With Sliding Mode Control for an Electric Vehicle in Urban Traffic Networks

Gian Paolo Incremona and Antonella Ferrara

Abstract— **This paper deals with an eco-driving control problem for autonomous electric vehicles in urban traffic networks with signalized intersections. Specifically, a novel control scheme is proposed to make the vehicle travel through a sequence of signalized intersections while always catching green lights with minimum energy consumption. The proposal includes a speed reference generator, a sliding mode local controller and an event-triggered decision maker whose intelligence is provided by a pre-specified condition. This mechanism enables to determine when it is necessary to re-plan a new optimal velocity profile by the speed planner, which solves a sub-optimal version of the non-convex eco-driving optimal control problem due to the traffic lights constraints. The sliding mode controller instead enables a finite time tracking of the optimized speed reference and plays the role of compensator of the uncertainties affecting the vehicle dynamics. Such a robustness property in turn allows to limit the triggering events when a new optimization is solved to update the speed reference profile. The performance of the whole control scheme are finally assessed in simulation.**

Index Terms— **Eco-driving control, sliding mode control, event-triggered control, optimization.**

I. Introduction

Environmental protection and ecological transition are currently at the center of the political agenda in order to promote innovative technological solutions of the energy sector, including sustainable mobility [1]. In this context, transportation represents one of the main contributors to pollution and carbon emissions, so that many companies are investigating on opportunities and strategies to decrease energy consumption in order to be sustainable and more profitable in the future.

Though in general railway vehicles are the most efficient means of transportation from the point of view of energy consumption (see e.g., [2], [3]), many studies and experimental tests of traffic control systems for conventional vehicles have been realized over the last decades, see [4]. Traffic congestion in urban or freeway networks has in fact a strong impact on the environment and the society, causing the formation of jams, and increasing travel times of users with consequences for productivity, safety, and pollution. Health risks due to vehicle emission have been deeply studied [5], also considering their relationship with travel times and duration of rush hours. In the literature many control approaches have been proposed ranging from Variable Speed Limits (VSL) to Ramp-Metering in freeway scenarios [6], [7], to eco-driving approaches locally applied to the vehicles (see e.g., [8], [9] among many others).

As for vehicle dynamics, indeed, while some methods are operator-based, thus requiring upgrade in the vehicle technology, others solutions are control-based. More precisely, eco-driving techniques usually refer to the application of strategies aimed at reducing energy consumption and carbon emissions acting on the driver behaviour (that is on the driving style), without necessarily modifying the vehicle technology. Such approaches can be classified into Driver Advisory Systems (DAS), if the driver is present, or they can be applied to fully autonomous vehicles. In both cases, a speed reference is generated as outcome of an optimal control problem subject to specific driving constraints. The latter are provided in order to limit road congestions, reduce sudden accelerations and decelerations, and to possibly avoid many stops at the traffic lights.

Among many works in the literature, in [10], [11], for instance, a switching formulation of the eco-driving control problem is adopted and a switched nonlinear Model Predictive Control is designed to solve the problem in presence of velocity, acceleration, emission and fuel consumption constraints. The minimization of the idle time is discussed in [12] together with emission and acceleration/deceleration limits. Specifically, the goal is to provide a suitable velocity profile to the driver in order to maximize the probability of catching green lights in urban traffic scenarios. Nowadays, this could be possible by virtue of Vehicle to Vehicle (V2V), and Vehicle to Infrastructure (V2I) communication technologies. In [13] an extensive discussion on motion planning methods for autonomous vehicles is reported, proposing an optimal multilane driving approach in dense traffic with traffic lights, adopting short planning horizons and decoupled or hierarchical solutions. In [14], instead, a sub-optimal approach capable of overcoming the non-convexity of constraints coming from the traffic lights is proposed in the case of DAS based vehicles in urban traffic networks. The optimal crossing time minimizing the energy consumption at each intersection is computed by creating a graph and selecting the feasible paths which comply with pre-specified speed limits.

Inspired by [14], and motivated by recent related traffic light systems already present in field, in this work we propose a novel control scheme for eco-driving of autonomous electric vehicles in urban traffic scenarios. The proposal consists

G. P. Incremona is with Dipartimento di Elettronica, Informazione e Bioingegneria, Politecnico di Milano, 20133 Milan, Italy (e-mail: *gianpaolo.incremona@polimi.it*). A. Ferrara is with Dipartimento di Ingegneria Industriale e dell'Informazione, University of Pavia, 27100 Pavia, Italy (e-mail: *antonella.ferrara@unipv.it*). The work of G. P. Incremona has been partially supported by the Italian Ministry for Research in the framework of the 2017 Program for Research Projects of National Interest (PRIN), Grant no. 2017YKXYXJ.

of three key elements: the speed reference planner, an event-triggered decision maker, and a sliding mode controller (SMC). The first one solves a sub-optimal version of the eco-driving control problem which is non-convex due to traffic light constraints. It finds the minimum-energy path within a predefined horizon without stops at traffic lights, and it updates the reference speed profile whenever a smart decision maker verifies a pre-specified triggering condition. Its intelligence is indeed provided by the capability of determining when it is necessary to re-plan the eco-path (that is the path with minimum energy) given the current state conditions of the vehicle. Finally, the sliding mode controller enhances the robustness properties of the scheme [15]. Indeed, not only ensures it finite time tracking of speed reference, but rejects possible uncertainties affecting the system. This has the effect of reducing the triggering events which enable a new optimization of the path, with beneficial effects in terms of communication reduction and computational burden with respect to classical controllers.

This work extends the results in [14], where only the speed planner is discussed for DAS based vehicles, to the case of an autonomous electric vehicle, whose dynamics is affected by unavoidable modelling uncertainties and disturbances. Such uncertain terms can significantly deviate the vehicle velocity from the desired speed profile, thus requiring a new optimization by the speed planner. The proposed novel architecture is capable of efficiently managing the speed re-planning, hence avoiding to frequently execute the optimization, and guarantees a finite time tracking of the reference, while fulfilling all the constraints due to the vehicle limits and traffic lights.

II. Problem Formulation

In this section the considered vehicle dynamics and the urban traffic scenario are described. Then, the eco-driving optimal control problem is formulated.

A. Vehicle modelling

Consider an electric vehicle with dynamics captured by the second-order kinematic model

$$\begin{cases} \dot{p}(t) = v(t) \\ m\dot{v}(t) = \frac{R_\mathrm{t}}{r}(T_\mathrm{m}(t) + d(t)) - F_\mathrm{loss}(v(t)), \end{cases} \tag{1}$$

where the longitudinal position of the vehicle is described along the 1-dimensional space coordinate p, while v is the velocity. The vehicle mass is denoted as m, while F_loss is a term including the aerodynamic drag force, the rolling resistance force, and the gravity force, described as

$$F_\mathrm{loss} = \frac{1}{2}\rho_\mathrm{a} A_\mathrm{f} c_\mathrm{d} v^2 + mgc_\mathrm{r} + mg\sin(\alpha(p)), \tag{2}$$

where ρ_a is the air density, c_d is the aerodynamic coefficient, c_r is the rolling resistance coefficient, A_f is the frontal surface, and g is the gravitational acceleration. Moreover, R_t is the gearbox transmission ratio, r is the wheel radius, and the demanded motor torque is instead T_m, affected by a disturbance term $d(t)$ (matched), which includes for instance unmodelled actuator dynamics as well as mismatches in the description of the losses. Such disturbance is assumed to be bounded, i.e., $\|d\|_\infty \leq \delta$, $\delta > 0$ being a suitably estimated bound.

Having in mind to include electric energy spare as a control objective, the adopted model for the electric power flow is

$$P_\mathrm{m} = V_\mathrm{a} i_\mathrm{a} = \omega_\mathrm{m} T_\mathrm{m} + \frac{R_\mathrm{a}}{\kappa^2} T_\mathrm{m}^2, \tag{3}$$

where V_a and i_a are the armature voltage and current, respectively, ω_m is the rotational speed of the motor, R_a is the armature resistance, and κ is the speed constant.

Now, exploiting the polynomial approximation

$$F_\mathrm{loss} = a_0 + mg\sin(\alpha(p)) + a_1 v + a_2 v^2,$$

with a_0, a_1, a_2 suitable estimated parameters (see [16] for further details), and letting

$$h_1 = \frac{R_\mathrm{t}}{mr},\ h_2 = \frac{a_2}{m},\ h_3 = \frac{a_1}{m},\ h_0 = \frac{a_0}{m} + g\sin(\alpha),$$

system (1) becomes

$$\begin{cases} \dot{p}(t) = v(t) \\ \dot{v}(t) = h_1(u(t) + d(t)) - h_2 v^2(t) - h_3 v(t) - h_0, \end{cases} \tag{4}$$

with input $u = T_\mathrm{m}$.

B. Traffic scenario

Let us consider an urban road stretch of length L without curves and with n traffic lights at the intersections located at p_i. The vehicle has to reach a final destination of coordinates $(t_\mathrm{f}, p_\mathrm{f})$, with $p_\mathrm{f} = p_{n+1}$, starting at (t_0, p_0), while fulfilling a pre-specified speed constraint

$$v_\mathrm{min} \leq v \leq v_\mathrm{max}, \tag{5}$$

with v_min and v_max being the corresponding bounds. As for the traffic lights and their green/red phase cycles, these are captured by the evolution of the state s_i, $i = 1, \ldots, n$, which is assumed deterministic and predefined, and given by

$$s_i(t) = \begin{cases} 1, & kT < t - \theta_i \leq kT + T_\mathrm{gr} \\ 0, & kT + T_\mathrm{gr} < t - \theta_i \leq (k+1)T, \end{cases} \tag{6}$$

where k indicates the number of cycles, T is the whole cycle length, $\theta_i \in [0, T)$ is the time offset of the ith intersection, and T_gr the duration of the green phase (i.e., $s_i = 1$).

C. Eco-driving control problem

We are now in a position to formulate the eco-driving control problem to solve. Letting $b_1 = R_\mathrm{t}/r$ and $b_2 = R_\mathrm{a}/\kappa^2$ be two constant weights, we define as eco-driving control the solution of the power consumption minimization problem

$$\begin{aligned} \min_u J = \int_{t_0}^{t_\mathrm{f}} & b_1 uv + b_2 u^2 \,\mathrm{d}t \\ \text{s.t.} \quad & (4),\ (5), \\ p(t_0) = p_0, & \quad p(t_\mathrm{f}) = p_\mathrm{f}, \\ p(t_i) = p_i & \wedge s_i(t_i) = 1, \\ v(t_0) = v_0, & \quad v(t_\mathrm{f}) = v_\mathrm{f}, \end{aligned} \tag{7}$$

subject to the nominal evolution of the system, that is $d = 0$ in (4), with v_0 and v_f being the desired initial and final velocities, respectively. Note that the key difficulty in solving (7) is given by the presence of the constraint $p(t_i) = p_i \wedge s_i(t_i) = 1$, which can be given by disjoint sets because of multiple available green windows at the same intersection, thus resulting in a non-convex set. Moreover, since the real vehicle is actually affected by $d \neq 0$, the control aim is to enforce the vehicle to reach the destination p_f on time, while fulfilling all the constraints in (7) in spite of the matched disturbance.

III. The Proposed Control Scheme

The control problem formulated in the previous section is solved in this paper by proposing the control scheme in Figure 1. It includes three main blocks: the speed reference planner, the decision maker with the event-triggered (ET) condition, and the sliding mode controller.

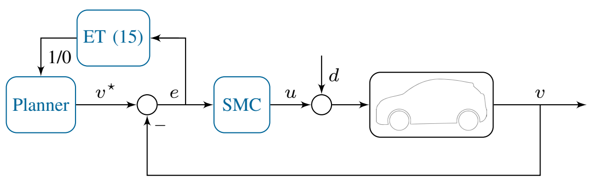

Fig. 1. The proposed control scheme.

A. Speed reference planner

In order to generate the optimal eco-driving based speed reference $v^\star$, the optimal control problem (7) is solved according to the procedure in [14]. Such technique allows indeed to simplify the previous non-convex problem by recasting it into sub-problems with convex constraints. It consists of the following three steps.

1) Pruning algorithm: In this step, taking into account the speed limits in (5), the algorithm (see [14, Sec. 3.1] for a detailed discussion) identifies the feasible region

$$\mathcal{P}_t := \{(t_{i,\min\,/\,\max}, p_i), | \quad s(t_{i,\min\,/\,\max}) = 1, \forall\, i = 1, \dots, n\}, \quad (8)$$

at the time instant t, where

$$t_{i,\min} = \frac{p_i - p_{i-1}}{v_{\max}} + t_{i-1,\min},\; t_{i,\max} = \frac{p_i - p_{i-1}}{v_{\min}} + t_{i-1,\max}.$$

Specifically, the region $\mathcal{P}_t$ is feasible in the sense that there exist paths catching always the green phases and complying with speed limits (5).

2) Dijkstra's algorithm: Given the feasible region $\mathcal{P}_t$, in this step the most energy efficient path from p_0 to p_f is selected among all the possible ones inside the region. Specifically, a weighted directed acyclic graph $\mathcal{G} = (\mathcal{V}, \mathcal{E})$ is realized with vertices belonging to $\mathcal{V}$, and set of edges equal to $\mathcal{E}$. Then a weighting function $w : \mathcal{E} \to E$ is defined in order to associate each edge with a weight based on travel energy cost, i.e.,

$$E = E_\ell + E_\mathrm{j}, \quad (9)$$

where

$$E_\ell = \Delta T(b_1 \bar{u}_i \bar{v}_i + b_2 \bar{u}_i^2) \quad (10)$$

is the energy contribution given by a constant velocity $\bar{v}_i = (p_i - p_{i-1})/\Delta T$, with $\bar{u}_i = (h_2 \bar{v}_i^2 + h_3 \bar{v}_i + h_0)/h_1$, and ΔT being the travel time between two vertices, while

$$E_\mathrm{j} = \int_0^{t_\mathrm{j}} b_1 u v + b_2 u^2 \mathrm{d}t \quad (11)$$

is the contribution when there is a change of velocity at a node between two edges, with $t_\mathrm{j} = |v_{i+1} - v_i|/a$, a being a fixed acceleration such that $v = v_i \pm at$, for $i = 0, \dots, n+1$. Note that, as discussed in [14, Sec. 3.2], such approximation can imply some difficulty in assigning the energy contribution, and a decoupling of the nodes should be applied. Finally, the so-called Dijkstra's algorithm is adopted to find the minimum energy trip.

3) Optimal path: The last step consists in the solution of the eco-driving optimization, which is recast into a suitable convex form. More precisely, to do it, let $\mu = [t_1, \dots, t_n]' \in \mathbb{R}^n$ be the new optimization variables vector, so that the vector of constant velocities between two intersections is

$$\nu(\mu) = [v_1, \dots, v_{n+1}]' = \left[\frac{p_1 - p_0}{t_1 - t_0}, \dots, \frac{p_{n+1} - p_n}{t_\mathrm{f} - t_n}\right]',$$

and the cost function in (7) can be rewritten as

$$J(\mu) = [t_1 - t_0, \dots, t_\mathrm{f} - t_n] P(\nu) + \sum_{i=0}^{n+1} E_\mathrm{j}, \quad (12)$$

where $P(\nu) = b_1 \bar{u}(\nu)\nu + b_2 \bar{u}^2(\nu)$, with

$$\bar{u}(\nu) = \frac{h_2 \nu^2 + h_3 \nu + h_0}{h_1}.$$

Hence, the eco-driving control problem (7) is recast into

$$\min_{\mu} J(\mu) \quad (13)$$
$$\text{s.t. } \max\{t_i^-, t_{i,\min}\} \le t_i \le \min\{t_i^+, t_{i,\max}\},\ \forall i = 1, \dots, n,$$

where t_i^- and t_i^+ are the end times of the selected green phase at each intersection. Finally, taking into account the outcome solution $\mu^\mathrm{o} = [t_1^\mathrm{o}, \dots, t_n^\mathrm{o}]'$ and the corresponding vector $\nu^\mathrm{o}(\mu^\mathrm{o})$, a suitable piecewise constant speed reference is generated as

$$v^\star(t) = v_{i+1}^\mathrm{o}, \quad \forall\, t \in [t_i, t_{i+1}),\ i = 0, \dots, n. \quad (14)$$

B. Event-triggered re-planning

Since the actual velocity of the vehicle can deviate from the desired one, a new optimization could be necessary. Therefore, the decision maker reported in Figure 1 plays the role of measuring the velocity error, and of determining a new optimization by the planner provided that an ET condition holds. Let $\{t_j\}_{j \in \mathbb{N}_{\ge 0}}$ be the sequence of the triggering instants, generated such that

$$t_{j+1} := \inf\{t > t_j \mid \mathcal{T}_1(e(t)) \ge 0 \wedge \mathcal{T}_2(t_{j-1}) \ge 0 \wedge \mathcal{T}_3(p_i) \ge 0, \forall\, i = 1, \dots, n\}, \quad (15)$$

where $\mathcal{T}_1$, $\mathcal{T}_2$ and $\mathcal{T}_3$ are suitably selected event functions. Specifically, the first one depends on the velocity error with respect to its reference, namely $e(t) = v^\star(t) - v(t)$, that is

$$\mathcal{T}_1(e(t)) = |e(t)| - \varepsilon_v, \tag{16}$$

with $\varepsilon_v > 0$ being a design threshold parameter. The second term represents instead a dwell-time condition to avoid frequent triggering instances, and it is given by

$$\mathcal{T}_2(t_{j-1}) = t - t_{j-1} - \varepsilon_\tau, \tag{17}$$

with $\varepsilon_\tau > 0$ being the minimum waiting time. Finally, the last one is a term related to a minimum distance between the vehicle and the next intersection position p_i, $\forall\, i = 1, \dots, n$, i.e.,

$$\mathcal{T}_3(p_i) = p_i - p(t) - \varepsilon_p, \tag{18}$$

with $\varepsilon_p > 0$ being a suitable selected threshold. Therefore, whenever a new event occurs, a flag equal to 1 is sent to the speed reference planner in order to enable a new optimization, given the updated initial conditions $t_0 = t_j$ and $p_0 = p(t_j)$.

C. Sliding mode controller

Given the reference $v^\star$ generated by the planner, the use of a SMC is motivated by the presence of unavoidable modelling uncertainties and disturbances affecting the system (the matched term d in our case). Indeed, it is well known that the SMC is capable of making the controlled system insensitive to bounded matched uncertainty terms. Without loss of generality, since the system output corresponds to the vehicle speed, the relative degree is equal to 1, hence a first order SMC naturally applies. Specifically, let the so-called sliding variable σ be equal to the speed error, i.e, $\sigma(t) = e(t)$. Then, the sliding mode control law is designed as $u(t) = u_0(t) + u_1(t)$, where u_0 is a feed-forward term to compensate the known dynamics, that is

$$u_0(t) = \frac{h_2 v^2(t) + h_3 v(t) + h_0}{h_1}, \tag{19}$$

while u_1 is the discontinuous component given by

$$u_1(t) = K\,\mathrm{sign}(\sigma(t)), \tag{20}$$

with $K > \delta$ being the control gain to enforce in a finite time a sliding mode on the manifold $\sigma \equiv 0$ for any $t \geq \bar{t}$, where $\bar{t}$ is the reaching time. Such a condition can be proved by choosing the function $V = 0.5\sigma^2$, and, according to the so-called *equivalent control* [17], namely $\tilde{u}$, by posing $\dot{\sigma} = 0$, one can prove that $\tilde{u}(t) = -d(t)$, that is the matched uncertainty terms are compensated when the sliding mode $\sigma \equiv 0$ is enforced. Moreover, note that an alternative approach to the discontinuous control law in (20) is represented by higher-order sliding mode controllers of suitable order and aimed at chattering alleviation.

IV. Case Study

In this section, the benchmark example in [14] is used to assess in simulation the proposed control scheme.

A. Settings

The considered scenario presents an urban road stretch of length $L = 2000\,\mathrm{m}$ with $n = 5$ intersections. In analogy with [14], the simulation parameters of the vehicle and of the considered scenario are reported in Table I. The control goal is to make the vehicle follow the speed reference $v^\star$ generated by the planner in spite of uncertainties injected in the vehicle dynamics in order to simulate possible mismatches due to modelling approximations or external forces from actuators. More precisely, the considered disturbance is a shifted low-frequency sinusoid with a random noise $\epsilon(t)$ superimposed (see e.g., [18]), i.e.,

TABLE I

Setting parameters

Vehicle		Scenario	
m	$1190\,\mathrm{kg}$	T	$30\,\mathrm{s}$
r	$0.2848\,\mathrm{m}$	T_{gr}	$10.8\,\mathrm{s}$
R_{t}	$6.066\,\Omega$	$\theta_{1\dots,n}$	$[13, 3, 28, 15, 5]\,\mathrm{s}$
a	$1.5\,\mathrm{m\,s^{-2}}$	$p_{1\dots,n}$	$[3, 6, 9, 12, 15.5] \times 10^2\,\mathrm{m}$
α	$0\,\mathrm{rad}$	p_{n+1}	$2000\,\mathrm{m}$
a_0	$113.5\,\mathrm{N}$	t_{f}	$200\,\mathrm{s}$
a_1	$0.774\,\mathrm{N\,m^{-1}\,s^{-1}}$	v_{f}	$13\,\mathrm{m\,s^{-1}}$
a_2	$0.4212\,\mathrm{N\,m^{-1}\,s^{-2}}$	$v_{\min}$	$5\,\mathrm{m\,s^{-1}}$
b_2	$0.1515\,\Omega$	$v_{\max}$	$14\,\mathrm{m\,s^{-1}}$

$$d(t) = \beta_1 + \beta_2 \left[\sin\left(\frac{t}{\beta_3} + \beta_4\right) + \epsilon(t)\right], \tag{21}$$

with constant $\beta_1 = 40$, $\beta_2 = 10$, $\beta_3 = 10$, $\beta_4 = 0.5$ and $\epsilon(t) \in [0, 0.1]$, such that $\delta = 51$. Let $v(0) = 13.5\,\mathrm{m\,s^{-1}}$ be the initial velocity condition. The thresholds for the ET block are chosen as $\varepsilon_v = 0.2\,\mathrm{m\,s^{-1}}$ for condition $\mathcal{T}_1$ in (16), $\varepsilon_\tau = 2\,\mathrm{s}$ for condition $\mathcal{T}_2$ in (17), and $\varepsilon_p = 10\,\mathrm{m}$ for condition $\mathcal{T}_3$ in (18). As for the SMC, the control gain is selected as $K = 60$.

B. Simulation results

The considered scenario with the green and red phases of traffic lights is illustrated in Figure 2. Moreover, in the same figure, it is possible to observe the feasible region $\mathcal{P}_0$ (solid gray line) generated at $t = 0$, and the re-planned regions $\mathcal{P}_{t_j}$ (dashed gray lines) at the triggering instants $t = t_j$ determined by condition (15). The time evolution of the planned position profile (solid blue line) is also reported, while in Figure 3 the time evolution of the vehicle speed is illustrated. As expected, the SMC allows to track in finite time the desired speed reference, and, although the sliding mode $\sigma \equiv 0$ (that is $v = v^\star$) is sometimes lost due to the step variations of the reference, the sliding phase is reached again in a finite time in spite of the disturbance affecting the system. The error evolution is given in Figure 4, together with the boundary layer of size ε_v representing condition (16). The flag signals provided by the decision maker to the planner are instead visualized in Figure 5.

C. Comparison

We conclude this section with a comparison of the proposed SMC based scheme with another available option. As

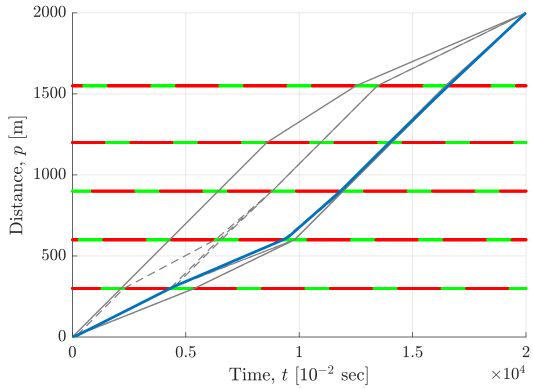

Fig. 2. Sub-optimal path (solid blue line), feasible region $\mathcal{P}_0$ (solid gray line) and re-planned ones (dashed gray lines) at each t_j if (15) holds, when the SMC is used.

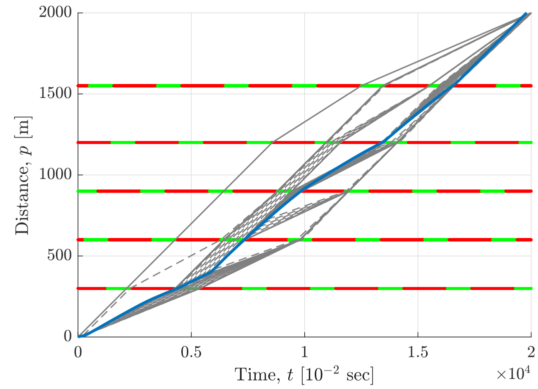

Fig. 6. Sub-optimal path (solid blue line), feasible region $\mathcal{P}_0$ (solid gray line) and re-planned ones (dashed gray lines) at each t_j if (15) holds, when the PD control is used.

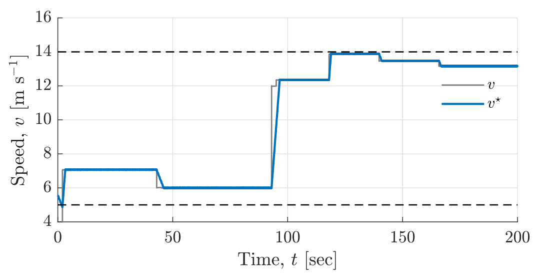

Fig. 3. Time evolution of the velocity $v(t)$ (solid blue line) with respect to its reference $v^\star(t)$ (solid gray line), when the SMC is used.

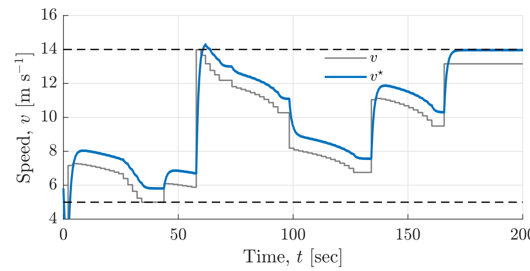

Fig. 7. Time evolution of the velocity $v(t)$ (solid blue line) with respect to its reference $v^\star(t)$ (solid gray line), when the PD control is used.

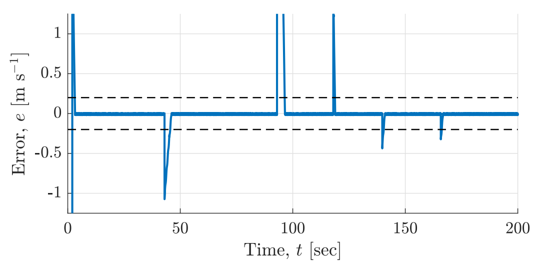

Fig. 4. Time evolution of the error $e(t)$ (solid blue line), and boundary layer of size ε_v (dashed black lines), when the SMC is used.

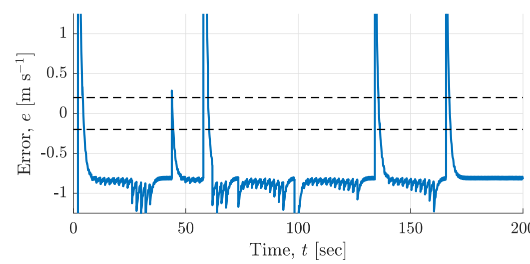

Fig. 8. Time evolution of the error $e(t)$ (solid blue line), and boundary layer of size ε_v (dashed black lines), when the PD control is used.

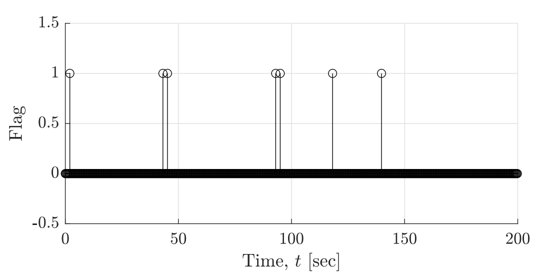

Fig. 5. Flag signals at the triggering instants t_j given by (15), when the SMC is used.

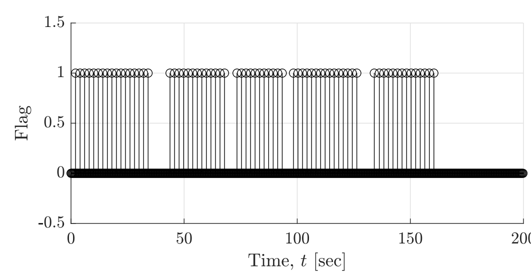

Fig. 9. Flag signals at the triggering instants t_j given by (15), when the PD control is used.

discussed in §II-C, one of the motivations for the use of the ET approach is to reduce as much as possible the number of updates of the speed reference when the disturbance causes a significant deviation of the vehicle velocity from the desired one. Furthermore, this aspect is the incentive for adopting the SMC technique, which is well-known for its robustness in front of matched uncertainties. Therefore, it makes sense to compare the proposed scheme with a classical PD controller. Our comparison criteria are:

1) the the root mean square of the control input u, termed iRMS;
2) the disturbance attenuation performance, measured by the

root mean square error $e(t)$, termed RMSe;

3) the number of triggering events when a new re-planning phase is activated, indicated as #flag.

The considered PD control has proportional and derivative gains $K_{\mathrm{P}} = 50$ and $K_{\mathrm{d}} = 1$, respectively, tuned to obtain a satisfactory behaviour of the controlled system, such that the speed error is comparable to the one achieved with SMC.

TABLE II
PERFORMANCE WHEN SMC AND PD CONTROL ARE ADOPTED.

	ε_v	0.1	0.2	0.3	0.5	0.8
	ε_τ	1	2	3	4	5
SMC	iRMS	54.67	55.29	54.98	55.23	54.69
	RMSe	1.84	0.68	2.07	1.03	1.4
	#flag	27	7	11	4	6
PD	iRMS	51.51	57.48	50.82	60.01	52.25
	RMSe	1.13	1.23	1.11	1.27	1.14
	#flag	136	70	47	35	28

The results reported in Table II show that SMC allows to considerably reduce the number of updates (11 on average) of the speed reference, while maintaining the average RMSe around $1.4\,\mathrm{m\,s^{-1}}$. It is worth to highlight that, although apparently the RMSe with PD control is 16% smaller on average, the number of triggering events is considerably higher (63 updates versus 11 achieved with SMC on average). This aspect is indicative of the fact that the error is maintained inside the layer for a longer time window when the SMC is adopted, thus confirming its robustness in front of the considered disturbance. As for the control effort the two strategies are comparable. Figure 6 reports the sub-optimal path achieved according to the algorithm discussed in §III-A, together with all the re-planned feasible regions $\mathcal{P}_t$, when the PD control is used under the same conditions, i.e., $\varepsilon_v = 0.2\,\mathrm{m\,s^{-1}}$, $\varepsilon_\tau = 2\,\mathrm{s}$, and $\varepsilon_p = 10\,\mathrm{m}$. In this case, the velocity profile presents several variations which influence the eco-driving style more than in the case of the proposed SMC (see Figure 2). In Figure 7 the actual velocity of the vehicle and its reference are illustrated, and the corresponding error is shown in Figure 8. Finally, Figure 9 illustrates the corresponding flag signals in a number greater than the one obtained with SMC. Indeed, the latter keeps the error more confined inside the layer defined by condition (16).

V. CONCLUSIONS

The problem of eco-driving for a vehicle in urban traffic network in presence of signalized intersections is addressed in this paper. Specifically, an event-triggered mechanism is adopted to re-plan the speed reference achieved as output of an optimization problem. Inspired by [14], such minimization allows the reduction of energy consumption while making the vehicle always catch a green light sequence. The local controller of sliding mode type allows to guarantees a finite time tracking of the speed reference in spite of possible uncertainties affecting the system. Differently from classical PD control approaches, the enhanced robustness due to the SMC allows to considerably reduce the number of triggering events which determine new optimizations in order to update the vehicle speed reference.

Future works will be devoted to the design of higher order sliding mode controllers aimed at chattering alleviation, and the application to the multi-vehicle scenario.

VI. ACKNOWLEDGMENTS

The authors gratefully acknowledge the help provided by the master student Fabio Banfi for the simulation tests.

REFERENCES

[1] Energy transition & climate sustainability working groups, "Joint G20 energy-climate ministerial communiqué," [Accessed: 1-11-2021], source: https://www.g20.org/wp-content/uploads/2021/07/2021_G20-Energy-Climate-joint-Ministerial-Communique.pdf.

[2] Q. Gu, T. Tang, F. Cao, and Y.-d. Song, "Energy-efficient train operation in urban rail transit using real-time traffic information," *IEEE Transactions on Intelligent Transportation Systems*, vol. 15, no. 3, pp. 1216–1233, Jun. 2014.

[3] H. Farooqi, G. P. Incremona, and P. Colaneri, "Railway collaborative ecodrive via dissension based switching nonlinear model predictive control," *European Journal of Control*, vol. 50, pp. 153–160, Nov. 2019.

[4] A. Hegyi, T. Bellemans, and B. De Schutter, *Freeway Traffic Management and Control*. New York, NY: Springer New York, 2009, pp. 3943–3964.

[5] K. Zhang and S. Batterman, "Air pollution and health risks due to vehicle traffic," *Science of the Total Environment*, vol. 450–451, pp. 307–316, Apr. 2013.

[6] A. Ferrara, S. Sacone, and S. Siri, "An Overview of Traffic Control Schemes for Freeway Systems," in *Freeway Traffic Modelling and Control*. Springer, 2018, ch. 8, pp. 193–234.

[7] A. Ferrara, G. P. Incremona, and G. Piacentini, "A hierarchical MPC and sliding mode based two-level control for freeway traffic systems with partial demand information," *European Journal of Control*, vol. 59, pp. 152–164, May 2021.

[8] M. S. Alam and A. McNabola, "A critical review and assessment of Eco-Driving policy & technology: Benefits & limitations," *Transport Policy*, vol. 35, pp. 42–49, Sep. 2014.

[9] A. Sciarretta, G. De Nunzio, and L. L. Ojeda, "Optimal ecodriving control: Energy-efficient driving of road vehicles as an optimal control problem," *IEEE Control Systems*, vol. 35, no. 5, pp. 71–90, Oct. 2015.

[10] P. Polterauer, G. P. Incremona, P. Colancri, and L. del Re, "A switching nonlinear MPC approach for ecodriving," in *American Control Conference*, Philadelphia, PA, USA, Jul. 2019, pp. 4608–4613.

[11] G. P. Incremona and P. Polterauer, "Design of a switching nonlinear MPC for emission aware ecodriving," *IEEE Transactions on Intelligent Vehicles*, 2022, doi: 10.1109/TIV.2022.3140484.

[12] S. Mandava, K. Boriboonsomsin, and M. Barth, "Arterial velocity planning based on traffic signal information under light traffic conditions," in *12th IEEE International Conference on Intelligent Transportation Systems*, St. Louis, MO, USA, Sep. 2009, pp. 1–6.

[13] Z. Ajanovic, "Towards superhuman autonomous vehicles," Ph.D. dissertation, Technische Universitat Graz, 2019.

[14] G. De Nunzio, C. C. de Wit, P. Moulin, and D. Di Domenico, "Eco-driving in urban traffic networks using traffic signals information," *International Journal of Robust and Nonlinear Control*, vol. 26, no. 6, pp. 1307–1324, Apr. 2016.

[15] A. Ferrara, G. P. Incremona, and M. Cucuzzella, *Advanced and Optimization Based Sliding Mode Control: Theory and Applications*. Philadelphia, PA: SIAM, 2019.

[16] W. Dib, A. Chasse, P. Moulin, A. Sciarretta, and G. Corde, "Optimal energy management for an electric vehicle in eco-driving applications," *Control Engineering Practice*, vol. 29, pp. 299–307, Aug. 2014.

[17] V. I. Utkin, *Sliding Modes in Control and Optimization*, ser. Communication and control engineering. Springer-Verlag, 1992.

[18] M. Zambelli and A. Ferrara, "Robustified distributed model predictive control for coherence and energy efficiency-aware platooning," in *American Control Conference*, Philadelphia, PA, USA, Jul. 2019, pp. 527–532.